Self-Assembly of a Designed Protein Polymer into β-Sheet Fibrils and Responsive Gels

Nichole L. Goeden-Wood, Jay D. Keasling, and Susan J. Muller*

Department of Chemical Engineering, University of California−Berkeley, Berkeley, California 94720-1462

Received December 11, 2002; Revised Manuscript Received February 16, 2003

ABSTRACT: An artificial gene encoding the amino acid repeat sequence $(AEAEAKAKAEAEAKAK)_9$ was constructed and expressed in *E. coli*. affording a 17 236 Da His-tagged fusion protein, poly-EAK9. Circular dichroism and FTIR results suggest that poly-EAK9 adopts an extended β-strand conformation in an antiparallel β-sheet supramolecular aggregate. The structure appears highly stable and resistant to denaturation up to 6 M urea and over a range of pH and temperature conditions. Congo Red dye-binding assays support the presence of amyloid-like fibrils, and scanning electron microscopy studies confirm that these supramolecular structures are in fact smooth, well-defined fibrils, approximately 10−20 nm in diameter. Triggered gelation occurs under physiological conditions, suggesting the potential use of poly-EAK9 gels as biocompatible and biodegradable materials. Rheological and SEM experiments are consistent with the formation of an entangled polymer network, in which the polymer mesh size appears to be inversely related to protein concentration. Rheological measurements indicate that the material is significantly more elastic than a lower molecular weight synthetic peptide of the same structure. These results demonstrate that a high molecular weight, biosynthetic protein polymer of minimal complexity can be designed to self-assemble in solution to form β-sheet fibrils and transparent, self-supporting gels.

Introduction

Molecular self-assembly has recently drawn attention in the development of supramolecular structures and functional materials. In nature, we observe many examples of molecular self-assembly involving the spontaneous self-association of molecules into structurally well-defined architectures on mesoscopic to macroscopic length scales.[1] In particular, the biological β-sheet motif has received considerable attention for its self-assembling properties, including amyloid formation and its role in pathogenesis, and as a building block in the design of supramolecular materials such as peptide filaments, films, nanotubes, and crystals.[2−7] Such unique structure and functionality are a result of the amino acid sequence, stereochemistry, and the ability to control the polymer chain length and its polydispersity. For this reason, protein-like self-assembly has become a popular new strategy in polymer science and engineering for the synthesis of novel nanostructured materials. Although recent progress has been made in living polymerization techniques,[8,9] the two most common methods of amino acid polymer synthesis include Fmoc-based solid-phase peptide synthesis and recombinant protein production in a heterologous host.[1] Short synthetic peptides (∼7−40 aa) have contributed greatly to our understanding of β-sheet assembly and supramolecular organization.[6,10] However, significantly less work has been done on the production and characterization of high molecular protein polymers of minimal complexity that can undergo self-assembly. The use of a biosynthetic approach allows us to design and produce high molecular weight polymers that exceed the limits of sequential peptide synthesis (∼40 aa). This approach has proven particularly advantageous in the production of silk and elastin-like polymers and in the modular design of artificial protein polymers (e.g., multiblock copolymers).[1,2,11−16]

We previously described the construction and bacterial expression of a multimeric gene encoding the polymer, poly-EAK9 (17 236 Da), composed of an N-terminal Histidine tag for affinity purification and the "EAK" amino acid repeat sequence, $(AEAEAKAKAE-AEAKAK)_9$ (A = alanine, E = glutamate, K = lysine).[17] The synthesis and characterization of poly-EAK9 are of particular interest in studying the self-assembly of amphiphilic protein polymers. Sequences that contain alternating polar and nonpolar residues are known to adopt stable β-sheet structures and make up the most prevalent binary pattern found in antiparallel β-strands in natural proteins.[18] Previous studies of amphiphilic peptides, such as poly-Tyr-Glu and poly-Val-Lys, have demonstrated a tendency to aggregate over time or with changes in pH, salt concentration, or solvent conditions.[19,20] More recently, Dobson and co-workers have suggested a generic tendency of proteins to undergo fibril formation via the formation of a β-sheet hydrogen-bonding network along the polypeptide backbone.[21] The stability, solubility, and conformational properties of β-sheet fibrils, however, are inherently sequence dependent as side-chain specific interactions determine the physical and structural properties of the resulting fibrils. Earlier studies by Zhang and co-workers using short synthetic peptides of sequence $(AEAEAKAK)_2$ demonstrated the formation of an organized supramolecular structure in the presence of monovalent metal ions which was extremely resistant to denaturation and proteolytic degradation.[22] Such structural assembly and stability are due to the binary pattern of polar/nonpolar residues and the favorable side-chain packing and interactions (e.g., hydrophobic interactions along one face of the β-sheet and electrostatic interactions along the opposite side of the β-sheet). With a goal toward producing a stable, self-assembling polymer for advanced material applications, the "AEAEAKAK" amino

* To whom all correspondence should be addressed: e-mail muller2@socrates.berkeley.edu.

10.1021/ma025952z CCC: $25.00
Published on Web 03/27/2003

acid motif was chosen as the building block for the biosynthetic production of a high molecular weight analogue, poly-EAK9. The protein polymer's conformation and self-assembly are characterized by circular dichroism spectroscopy, Congo Red dye binding assays, and FTIR spectroscopy. The morphology and dimensions of the polymer supramolecular structures are established by scanning electron microscopy, and the mechanical properties of the resulting gels are obtained by rheological measurements.

Experimental Section

Materials. We previously described the construction and expression of a multimeric gene of 504 base pairs encoding the protein polymer, poly-EAK9 (17 236 Da), as a C-terminal fusion to the decahistidine tag (2785 Da) in pET19b (Novagen, Inc.).[17] Inducible expression of the multimeric gene in bacterial cultures of recombinant *Escherichia coli* strain BL21(DE3) afforded ~5 mg of poly-EAK9 per 1 L culture following purification by immobilized metal affinity chromatography, dialysis, and lyophilization. Amino acid analysis, N-terminal sequencing, and MALDI−TOF mass spectrometry analysis confirmed the sequence (shown below) and the molecular weight of poly-EAK9. Although the decahistidine tag can be removed via cleavage with cyanogen bromide, we found that the presence of the tag did not inhibit fibril assembly and subsequent gelation, making the use of a short affinity tag for rapid purification even more attractive. All polypeptide concentrations were determined by quantitative amino acid analysis.

The amino acid sequence of poly-EAK9 is as follows: GHHHHHHHHHHSSGHIDDDDKHM**[AEAEAKAK-AEAEAKAK]$_9$**A.

Circular Dichroism Measurements. Circular dichroism (CD) spectra were recorded in the far-ultraviolet region (190−250 nm) using an AVIV 62DS spectrometer (Aviv Associates, Lakewood, NJ) and a 1.0 mm quartz cuvette. A sampling interval of 1 nm and an averaging time of 3 s were used in all experiments. Protein concentrations (0.625−7.4 μM) were obtained by dilution from a working stock solution of poly-EAK9 in water, in which the protein concentration was determined by quantitative amino acid analysis. During temperature ramp experiments (25−95 °C), samples were equilibrated for 1−10 min prior to measurement, with no noticeable difference in the CD spectra at longer equilibration times. The pH-adjusted protein samples and those containing denaturant were equilibrated overnight prior to CD analysis. All samples and buffers were passed through a 0.22 μm filter prior to use.

Congo Red Dye Binding Studies. The method of Klunk et al.[23] was used in the spectrophotometric analysis of Congo Red (CR) + poly-EAK9 binding studies. Briefly, a 100−200 μM stock solution of Congo Red (Sigma-Aldrich) was prepared in 0.22 μm filtered phosphate buffered saline (PBS, 10 mM phosphate buffer, 2.7 mM KCl, and 127 mM NaCl, pH 7.4) and 10% ethanol to prevent CR micelle formation. The concentration of the filtered CR stock solution was determined by measuring the absorbance at 505 nm (using a molar absorptivity of 5.93×10^4 AU/(cm M) as reported by Klunk et al.). Poly-EAK9 was dissolved in filtered PBS to a final concentration of 350−550 μg/mL and magnetically stirred at high rpm for 3 days (25 °C), resulting in a cloudy solution presumably due to fibril formation and aggregation. To maintain a homogeneous mixture, aliquots were removed while continuously stirring the stock solution. Protein samples (5−35 μg/mL) were incubated with Congo Red (1.8−6.1 μM) for 30 min prior to spectral analysis. The absorbance spectra of CR, poly-EAK9, and CR+poly-EAK9 were recorded using a Beckman DU 640 spectrophotometer in the wavelength scan mode (300−700 nm), with a 2 nm sampling interval.

FTIR Spectroscopy. Fourier transform infrared (FTIR) spectra were recorded on a Nicolet Magna 560 spectrometer purged with a continuous flow of N_2 gas and equipped with a CaF_2 window. Semidilute solutions of poly-EAK9 were prepared in water/phosphoric acid (pH 2, 150 μM) and hexafluoro-2-propanol (HFIP, 1.6 mM), and the spectra were collected at 25 °C with a spectral resolution of 2 cm^{-1}. Buffer spectra were recorded under identical conditions to those of the protein samples and subtracted from the protein spectra. A qualitative analysis of poly-EAK9's secondary structure was made by comparison of the FTIR spectra to known peaks in the amide I region (1600−1700 cm^{-1}) corresponding to the α-helix/disordered, β-turn, and β-sheet protein secondary structure.[24]

Electron Microscopy. Scanning electron microscopy was performed on a Hitachi S-5000 operating at 10 kV. Samples (0.5−1.5 mg/mL) were adsorbed to silicon chips with and without a 0.1% w/v poly-L-lysine coating. (The poly-L-lysine coating was found to have little effect on the sample morphology as observed by SEM.) Protein samples were incubated for 5 min and rinsed with 0.1 M sodium cacodylate buffer (pH 7.2). Fixation occurred in cacodylate buffer with 2% glutaraldehyde. Samples were microwave heated to 37 °C for 40 s, rinsed twice at room temperature with buffer (2.5 min incubation), and further fixed with 1% osmium tetroxide in cacodylate buffer. Samples were again microwave heated to 37 °C for 40 s and subsequently rinsed with buffer for 30 s at room temperature. Sample dehydration was achieved by sequential incubation in 50, 70, 90, and 100% ethanol and subsequent exchange with liquid CO_2 in a Tousimis AutoSamdri 815, series A, critical point drying apparatus. Using a Balzers High Vacuum Unit BAF 301, critical point dried samples were coated with platinum (1−2 nm) and carbon (12 nm) to enable both secondary electron and backscattering detection. Samples were stored in a desiccator when not in use. Although the fixation and dehydration procedure may have introduced some structural artifacts into the samples, the dramatic differences in the observed morphology between samples are assumed to be intrinsic to the materials as the sample preparation protocol was the same for all samples.

Rheology. A Rheometrics RMS-800 mechanical spectrometer with a cone-and-plate geometry (25 mm diameter, 0.1 rad cone) was employed for dynamic mechanical spectroscopy. A 75 μM protein solution (0.13 wt %) in 2% acetic acid (0.475 mL) was placed on the plate of the rheometer, and a stainless steel cone was lowered to a truncation height of 56 μm. The cone and the protein sample were subsequently surrounded by a cellulose dialysis membrane (Pierce, Inc.), and approximately 25 mL of 10 mM sodium phosphate buffer (final pH 7) was added to the plate holder, submerging the protein sample and allowing for buffer exchange through the cellulose membrane to induce gelation. A water bath was used to maintain the sample temperature at 25 °C, and the plate holder was sealed with aluminum foil to minimize evaporative losses. After equilibration for roughly 12 h, the dialysis membrane was removed and the torque and normal forces were zeroed, and the linear viscoelastic region was determined by strain sweep experiments at constant frequency (0.01−10 rad/s). The storage (G') and loss (G'') moduli were subsequently measured as a function of frequency, from 0.01 to 10 rad/s at constant strain (15%).

Results and Discussion

1. Dilute Solution Properties. a. Secondary Structure. Far-UV circular dichroism (CD) spectroscopy was used to measure the secondary structure of poly-EAK9 in aqueous solution. The CD spectra indicate a pure β-sheet structure, of the poly-L-lysine antiparallel type,[25,26] displaying a maximum near 195 nm and a single minimum at 218 nm (Figure 1). Although a slight decrease in the molar mean residue ellipticity is observed at 218 nm for the lowest protein concentration, poly-EAK9's secondary structure appears largely independent of concentration and is maintained even at the submicromolar level (0.625 μM). Poly-EAK9 displays surprisingly large values for the maximum (195 nm) and minimum (218 nm) ellipticities in the observed CD

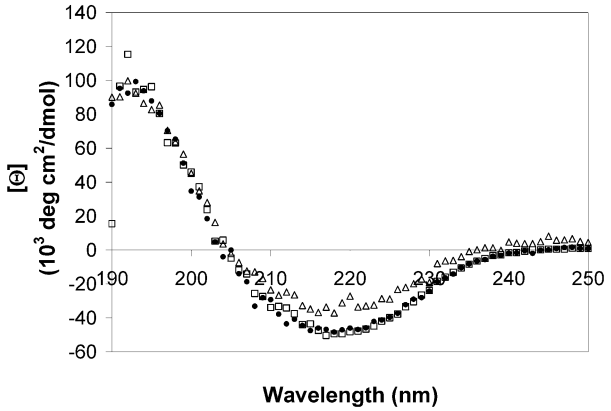

Figure 1. Poly-EAK9's β-sheet structure in water at 25 °C. CD spectra measured over a range of protein concentrations [(□) 2.5 μM, (●) 1.25 μM, and (△) 0.625 μM] demonstrate a high degree of structural stability even at submicromolar protein concentrations.

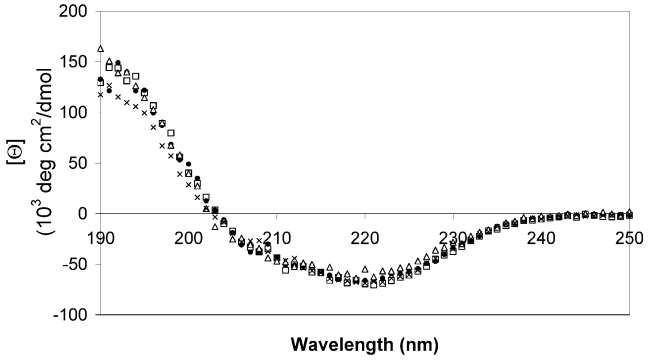

Figure 2. Poly-EAK9's (1.25 μM) structural stability over a range of pH. CD spectra (25 °C) measured at pH 11 (●), pH 8.4 (□), pH 5.6 (△), and pH 1.9 (×).

spectra. For example, the mean molar ellipticity per residue, Θ, at 218 nm is ∼−48 000 deg cm^2/dmol at protein concentrations ≥ 1.25 μM. In comparison, structurally well-defined β-sheets in natural proteins typically display Θ ∼ −10 000 deg cm^2/dmol,[10] and 16-residue synthetic peptides of similar sequence to poly-EAK9 display Θ ∼ −25 000 deg cm^2/dmol.[22,27,28] Large and negative CD signals near 218 nm appear characteristic of highly associated β-sheet structures,[29−31] suggesting a high degree of self-assembly in poly-EAK9's β-sheet structure even at low protein concentrations.

b. Structural Stability. The effect of pH, urea, and temperature on poly-EAK9's secondary structure was investigated to determine the material's structural stability under environmental stress. It was found that the β-sheet structure of poly-EAK9 is extremely resistant to denaturation over a wide range of temperature and solvent conditions. All spectra indicate a stable β-sheet structure from pH 1.9 to pH 11 (Figure 2). At pH 1.9, a lower CD signal is observed near the 195 nm region, possibly due to a change in the β backbone twist.[32] Such stability may be attributed to the ionic bonding between glutamate and lysine residues in the $i,i+4$ positions along the protein polymer chain as seen in synthetic EAK-based peptides with $i,i+4$ ionic interactions.[27,33] Since the pK_a of Glu and Lys residues are 4.4 and 10.0, respectively, it is likely that the β-sheet structure under highly basic or acidic conditions is stabilized by singly charged hydrogen bonds rather than ionic salt-bridges between the Lys and Glu residues.

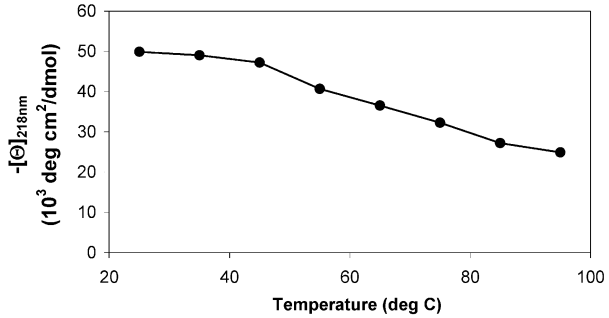

Figure 3. Thermal stability of poly-EAK9 (5 μM). The β-sheet structure is still present at 95 °C, although a 50% reduction in the molar mean residue ellipticity at 218 nm (−[θ] deg cm^2/dmol) was observed from 25 to 95 °C.

Poly-EAK9 also displays resistance to denaturation by urea. All spectra indicate a stable β-sheet structure in 2−8 M urea with no significant change in the ellipticity over the concentration range examined; the mean molar ellipticity at 218 nm remained constant at −23 000 deg cm^2/dmol. Compared to natural β-sheet proteins, which typically denature at concentrations above 4 M urea, poly-EAK9 shows a high degree of structural stability in the presence of a strong denaturing agent. It is interesting to note, however, that the ellipticity at 218 nm is approximately 50% of the value observed in water under similar conditions. Urea has been shown to disrupt β-sheet aggregation in amyloidic peptides, as observed by electron microscopy and circular dichroism.[34] Therefore, a change in the aggregation of the β-sheet structure may explain poly-EAK9's reduced ellipticity in urea at low protein concentrations.

The β-sheet structure of poly-EAK9 was also shown to be stable between 25 and 95 °C. A temperature ramp experiment was performed using equilibrated samples of poly-EAK9 in water, with a 10 °C sampling interval (Figure 3). As seen by the negative ellipticity at 218 nm, the β-sheet structure was maintained even as the temperature of the sample approached the boiling point of water. The ellipticity at 218 nm displayed an inverse dependence on temperature, suggesting minor conformational changes in poly-EAK9's β-sheet structure upon heating.

c. Congo Red Dye Binding Assay. To compare the quaternary structure of poly-EAK9 to other fibrillar β-sheet protein and peptide species, Congo Red binding studies were performed. Congo Red (CR) is a sulfonated diazo dye that binds preferentially, but not exclusively, to proteins and peptides exhibiting a cross-β-structure, characterized by β-sheet stacking perpendicular to the fibril axis.[30,31,35] To study poly-EAK9's quaternary structure under physiological salt and pH conditions, the protein was dissolved in filtered PBS buffer and subsequently stained with CR following the method of Klunk et al.[23] It was found that poly-EAK9 in PBS buffer forms aggregates which bind CR as evidenced by the characteristic hyperchromicity and red shift in the absorbance of the bound CR (Figure 4). Similar phenomena have been observed in insulin fibrils, the Alzheimer's β-peptide, and other amyloidic peptides.[23,30,36] CR has been used extensively as a histologic dye for amyloid protein detection, and the mechanism of CR interaction with β-sheet fibrils is currently under investigation. Electrostatic interactions between charged side chain residues and the sulfonate and amino groups of the dye along with intercalation of CR between

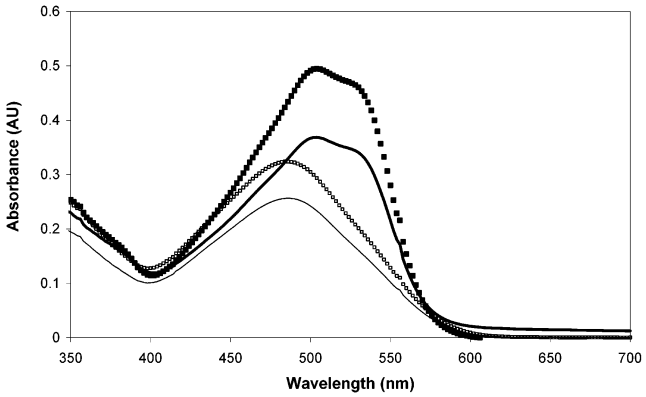

Figure 4. Shift of the Congo Red absorption peak on the addition of poly-EAK9. Absorbance spectra of unbound Congo Red (−, 4.6 μM; □, 6.1 μM) and Congo Red bound to 35 μg/mL (2 μM) poly-EAK9 in PBS buffer (−, 4.6 μM CR + poly-EAK9; ■, 6.1 μM CR + poly-EAK9).

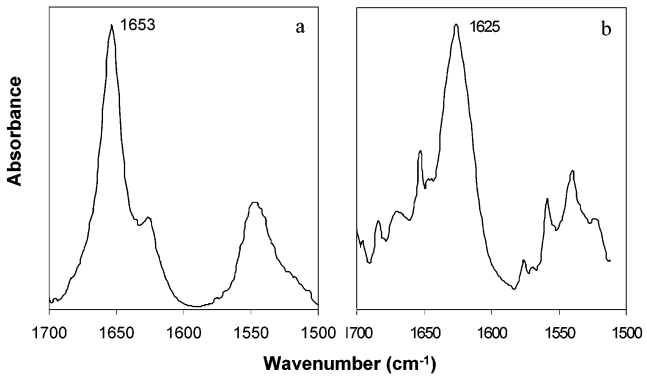

Figure 5. Fourier transform IR spectra of amide I (1700−1600 cm^{-1}) and amide II (1600−1500 cm^{-1}) bands of poly-EAK9 in (a) HFIP (1.6 mM) and (b) water, pH 2 (150 μM). Maximum amide I band at 1653 cm^{-1} is characteristic of an α-helical/disordered structure, whereas the peak at 1625 cm^{-1} corresponds to a β-sheet conformation.

protein molecules, protein β-sheet structure, and planarity requirements have been suggested as key factors in CR binding.[23,35,37−41] Although the structural specificity of CR binding is not yet known,[35,41] similarities in the CR dye binding studies of poly-EAK9 and well-characterized fibrillar β-sheet proteins suggest the presence of an ordered quaternary β-sheet structure in poly-EAK9 under physiological salt and pH conditions.

2. Semidilute Solution Properties. A key issue in controlling the self-assembly of poly-EAK9 into fibrils and gels was found to be protein solubility. We observed a strong tendency for poly-EAK9 to aggregate in most solvents we tested under semidilute protein concentrations (∼1−10 mg/mL). This is not surprising, as the polymer was designed to include strong side chain interactions and β-sheet hydrogen bonding to facilitate self-assembly. However, under conditions of low solubility, amorphous aggregates were observed which were resistant to subsequent solvation upon dilution. To determine the optimum solvent conditions for preparation of stock solutions, lyophilized protein was dissolved in a range of solvents including water with acetic acid (pH 3), water with phosphoric acid (pH 2), hexafluoro-2-propanol (HFIP), benzyl alcohol, and a denaturing buffer containing 8 M urea, 100 mM NaH_2PO4, and 10 mM Tris-Cl (pH 8) which was used in protein purification. Poly-EAK9 was found to be weakly soluble in benzyl alcohol (<1.75 mg/mL) and formed a transparent gel after 2 days in the urea denaturing buffer (protein concentrations > 300 μg/mL). Poly-EAK9 was moderately soluble at low pH (∼1−5 mg/mL) and even more soluble in HFIP (>20 mg/mL). At low pH, the Glu residues are protonated, resulting in a net positive charge that would disfavor protein self-assembly due to electrostatic repulsion. Self-assembly would also be disfavored in HFIP, a strong hydrogen bond donor, which has been shown to have a dramatic effect on β-sheet content, favoring the formation of random coil and α-helical conformations in a designed β-sheet peptide.[3] These observations were consistent with FTIR spectra of poly-EAK9 in HFIP and in water (pH 2). Poly-EAK9 in HFIP displayed a maximum amide I peak at 1653 cm^{-1} (Figure 5a), consistent with the presence of largely helical and/or disordered structures, while samples in water at low pH displayed a lesser peak at 1652 cm^{-1} and a new dominant amide I peak at 1625 cm^{-1}(Figure 5b), indicative of intermolecular β-sheet formation. The 1539 cm^{-1} peak in the amide II region (1500−1600 cm^{-1}) is also consistent with a β-conformation.[24,42,43]

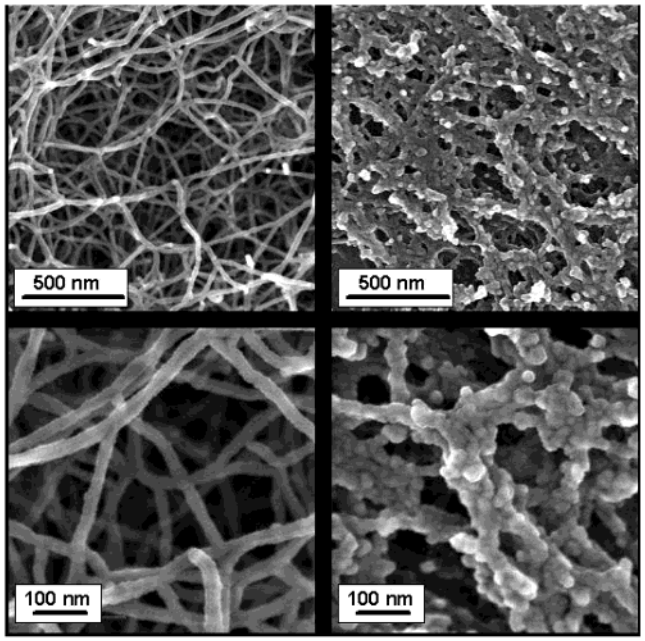

Figure 6. Morphology of poly-EAK9 in 2% acetic acid (30 μM, left) and benzyl alcohol (90 μM, right). SEM images are at 50 000× (first row) and 150 000× (second row) magnification.

a. Fibril Morphology. To study the microstructure of poly-EAK9 fibrils and gels, scanning electron microscopy was performed. Protein samples were incubated at room temperature approximately 1 week prior to SEM imaging. Many authors have reported slow kinetics during β-sheet fibril formation,[44−46] suggesting time scales from one to several weeks for obtaining equilibrium structures. We observed little difference in the morphology of poly-EAK9 fibrils equilibrated 1 week and those equilibrated for longer time periods, up to 1 month. Figure 6 illustrates the morphological features of poly-EAK9 in an aqueous, low-pH solvent (2% acetic acid) and an organic solvent (benzyl alcohol). Poly-EAK9 (30 μM) displayed smooth, well-defined fibrillar structures in 2% acetic acid. The fibrils appear to have a uniform diameter of approximately 10−20 nm. Although overlap of fibrils made it difficult to identify their ends and estimate their length, pieces of fibrils between points where they meet or cross were approximately

200−500 nm in length. Poly-EAK9 did not form ribbons or sheetlike arrays, as observed in several β-sheet peptides and proteins,[2,34,47] and the fibrils did not exhibit any clear axial substructures, such as helical twisting, transverse banding, or periodic coiling. Such uniform fibril morphology and dimensions, particularly the fibril diameter, suggest a highly stable structure that was reproducible between different protein samples prepared under similar conditions. In contrast, poly-EAK9 displayed a poorly defined morphology in benzyl alcohol (90 μM, Figure 6). Aggregates lacked the regular fibrillar morphology associated with amyloid-like structures, appearing as an inhomogeneous network of interconnected beaded filaments with nodular features. The unique microstructure of poly-EAK9 under aqueous and nonaqueous conditions was observed over a range of protein concentrations (30−100 μM) and is presumably the result of differences in the interactions between the protein and the solvent, highlighting the importance of the hydrophobic effect on uniform fibril assembly.

Interestingly, the small diameter of poly-EAK9 fibrils under aqueous conditions is not consistent with the extended β-strand length of poly-EAK9, predicted to be 56 nm (3.35 Å × 168 residues).[32] Although circular dichroism and FTIR experiments suggest that poly-EAK9 adopts an extended β-strand conformation in an antiparallel β-sheet supramolecular aggregate, the exact structure is unknown. In amyloid fibrils, X-ray fiber diffraction studies have revealed a characteristic "cross-β-structure", in which the β-strand of the precursor protein assembles perpendicular to the fibril axis via hydrogen bonding.[48] However, in addition to polymer chain length, the protein's secondary structural elements, helical twist, β-sheet packing, chain folding, and side chain interactions determine the resulting fibril diameter. It is interesting to note that several "EAK"-based materials are reported to have similar fibril diameters to those measured in poly-EAK9 fibrils. Zhang and co-workers observed fibrils with a 10−20 nm diameter following self-assembly of the synthetic peptide, $(AEAEAKAK)_2$.[22] Similarly, Conticello and co-workers observed 10−20 nm diameter fibrils (dispersed in a less structured matrix) following self-assembly of a 47 kDa silk-mimetic copolymer containing alternating $(AEAEAKAK)_2$ and $(GPGQQ)_6$ repeat units.[7] The apparent insensitivity of fibril diameter to polymer chain length has also been reported in amyloid fibrils, such as the Aβ(1−40) peptide implicated in Alzheimer's disease, the prion PrP^{SC}, and Transthyretin, which all appear as ∼10 nm diameter fibrils despite the range in peptide and protein chain lengths (20−127 residues).[49] Lack of three-dimensional information on how the β-strand precursor relates to overall fibril assembly is due in part to the difficulty in performing X-ray crystallography and NMR analysis of higher molecular weight fibrillar proteins.

b. Gel Properties. Poly-EAK9 was observed to gel upon equilibration in buffered salt solutions at neutral pH. Samples of poly-EAK9 in 2% acetic acid (∼1 mg/mL, 0.5 mL) were placed in dialysis cassettes (Pierce, Inc.) and incubated in sodium phosphate buffer (10 mM, pH 7.4) to induce gelation. After 30 min, the protein material formed a transparent, self-supporting gel that was stably maintained for weeks in solution. The microstructure of the protein gel was characterized by SEM and displayed a network of uniform, highly ordered fibrils (Figure 7). Similar fibril diameters (∼10−20 nm) were observed between the poly-EAK9 gels in 10 mM sodium phosphate buffer (90 μM, Figure 7) and the poly-EAK9 fibrils in 2% acetic acid (30 μM, Figure 6). However, at the higher protein concentration of the gelled samples, a more densely packed polymer network was observed, with a smaller mesh size of ∼100−200 nm.

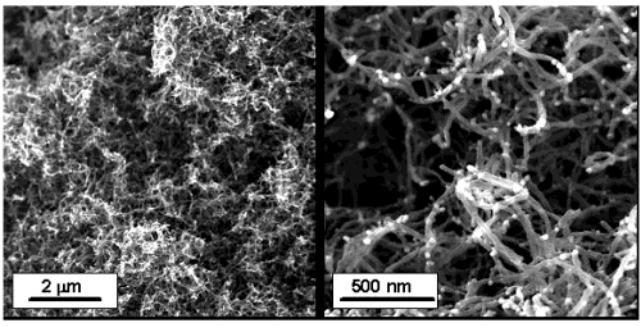

Figure 7. Morphology of poly-EAK9 gel (75 μM, 0.13 wt %) following incubation in 10 mM sodium phosphate buffer, pH 7.4. SEM images are at 10 000× (left) and 50 000× (right) magnification.

c. Dynamic Mechanical Properties. The dynamic mechanical spectrum of a typical poly-EAK9 gel (75 μM, 0.13 wt %) in 10 mM sodium phosphate buffer (pH 7.4) was obtained by small-strain oscillatory shear experiments. Following a 12 h incubation in the sodium phosphate buffer, a dramatic increase was observed in the storage modulus (data not shown). In the gel state, the storage modulus (G') was found to be an order of magnitude larger than the loss modulus (G''), indicative of an elastic material. G' and G'' appear to be essentially independent of frequency (ω) from 0.01 to 10 rad/s, suggesting a long relaxation time for the network which is not reflected in the measurements. Such dynamic mechanical behavior is characteristic of self-assembled polymers composed of long and entangled chains, which is consistent with poly-EAK9's microstructure as imaged by SEM (Figure 7). The long relaxation time of the polymer network is also consistent with the observation that the polymer gels were resistant to flow, following sample inversion. G' was approximately 50 Pa over the frequencies probed; higher storage moduli (>100 Pa) have been observed at higher protein concentrations (data not shown).

Dynamic mechanical properties of poly-EAK9 (168 residues) and the 16-residue synthetic peptide, $(AEAEAKAK)_2$, were also compared to determine the effect of polymer chain length on gel properties. Interestingly, under the same experimental conditions (0.1 wt % peptide in 10 mM sodium phosphate buffer, pH 7.4), the 16-residue synthetic peptide, AEAEAKAKAEAEAKAK, formed a much weaker gel than poly-EAK9. Even at a 10-fold higher molar concentration, the storage modulus (G') of the synthetic peptide gel is less than that observed in poly-EAK9 gels (Figure 8). Since the amino acid sequence of poly-EAK9 and the peptide are almost identical, except for the presence of poly-EAK9's N-terminal His tag, such differences in dynamic mechanical behavior are likely due to the differences in the polymer chain length, which can affect the strength of the hydrogen-bonding network and the side chain interactions that dictate the material properties of the resulting fibrils. Our findings suggest that polymer chain length may prove to be an important design

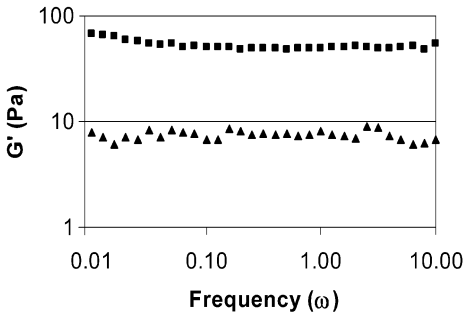

Figure 8. Comparison of the storage modulus (G') of (■) a poly-EAK9 gel (168 aa) and (▲) an EAK1 gel (16 aa). Samples at 0.1 wt % in 10 mM sodium phosphate buffer (22 °C) were examined by small-amplitude oscillatory shear in the linear viscoelastic region.

parameter in modulating the mechanical properties of self-assembling protein gels.

Conclusions

Understanding and controlling the self-assembly process of β-sheet polymers offers unique opportunities in the design of supramolecular structures for advanced material applications. In addition, the use of a biosynthetic approach to polymer synthesis allows precise control over the amino acid sequence and chain length in order to tune polymer mechanical properties. Here we have demonstrated that a high molecular weight, biosynthetic protein polymer of minimal complexity can be designed to self-assemble in solution to form β-sheet fibrils and transparent, self-supporting gels. Circular dichroism and FTIR results suggest that poly-EAK9 adopts an extended β-strand conformation in an antiparallel β-sheet supramolecular aggregate. The structure appears highly stable and resistant to denaturation over a broad range of temperature and solvent conditions. Congo Red dye binding assays support the presence of amyloid-like fibrils, and scanning electron microscopy studies confirm that these supramolecular structures are in fact smooth, well-defined fibrils, approximately 10−20 nm in diameter. Triggered gelation occurs under physiological conditions, suggesting the potential use of poly-EAK9 in biocompatible and biodegradeable material applications such as local drug delivery and soft-tissue replacement or as an extracellular matrix analogue. Rheological and SEM experiments are consistent with the formation of an entangled polymer network, in which the polymer mesh size appears to be inversely related to protein concentration.

By demonstrating that the N-terminal decahistidine tag does not inhibit gel formation, we have further illustrated the usefulness of this tag for high yield, affinity purification, of recombinant protein polymers. Further study is needed to characterize the effect, if any, the decahistidine tag has on gel properties and the effect of sequence design and polymer chain length on protein conformation, self-assembly, and stability. Further modulation of the mechanical properties of β-sheet polymer gels will likely result in a broad spectrum of novel properties and applications.

Acknowledgment. We gratefully acknowledge Professor Susan Marqusee for the use of the AVIV 62DS spectrometer, Professor Nitash Balsara for the use of the Nicolet Magna 560 FTIR spectrometer, and the UC Berkeley Electron Microscope Lab for the use of the Hitachi S-5000 scanning electron microscope. This work was supported by the UC Biotechnology Program, the National Science Foundation (BES-0103468), and a NSF Graduate Fellowship and UC Berkeley Dissertation Year Fellowship (N.L. Goeden-Wood).

References and Notes

(1) McGrath, K., Kaplan, D. S., Eds. *Protein-Based Materials*; Birkhäuser: Boston, 1997.
(2) Krejchi, M. T.; Atkins, E. D. T.; Waddon, A. J.; Fournier, M. J.; Mason, T. L.; Tirrell, D. A. *Science* **1994**, *265*, 1427−1432.
(3) Aggeli, A.; Bell, M.; Boden, N.; Keen, J. N.; McLeish, T. C. B.; Nyrkova, I.; Radford, S. E.; Semenov, A. *J. Mater. Chem.* **1997**, *7*, 1135−1145.
(4) Hartgerink, J. D.; Clark, T. D.; Ghadiri, M. R. *Chem.—Eur. J.* **1998**, *4*, 1367−1372.
(5) West, M. W.; Wang, W. X.; Patterson, J.; Mancias, J. D.; Beasley, J. R.; Hecht, M. H. *PNAS* **1999**, *96*, 11211−11216.
(6) Zhang, S. G.; Altman, M. *React. Funct. Polym.* **1999**, *41*, 91−102.
(7) Qu, Y.; Payne, S. C.; Apkarian, R. P.; Conticello, V. P. *J. Am. Chem. Soc.* **2000**, *122*, 5014−5015.
(8) Deming, T. *J. Polym. Sci., Part A: Polym. Chem.* **2000**, *38*, 3011−3018.
(9) Nowak, A. P.; Breedveld, V.; Pakstis, L.; Bulent, O.; Pine, D. J.; Pochan, D.; Deming, T. J. *Nature (London)* **2002**, *417*, 424−428.
(10) Nesloney, C. L.; Kelly, J. W. *Bioorg. Med. Chem.* **1996**, *4*, 739−766.
(11) Capello, J.; Ferrari, F. In *Plastics from Microbes*; Mobley, D. P., Ed.; Hanser/Gardner: Cincinnati, OH, 1994; p 35.
(12) McMillan, R. A.; Lee, T. A. T.; Conticello, V. P. *Macromolecules* **1999**, *32*, 3643−3648.
(13) Meyer, D. E.; Chilkoti, A. *Biomacromolecules* **2002**, *3*, 357−367.
(14) McPherson, D. T.; Morrow, C.; Minehan, D. S.; Wu, J. G.; Hunter, E.; Urry, D. W. *Biotechnol. Prog.* **1992**, *8*, 347−352.
(15) Prince, J. T.; McGrath, K. P.; Digirolamo, C. M.; Kaplan, D. L. *Biochemistry* **1995**, *34*, 10879−10885.
(16) Guda, C.; Zhang, X.; McPherson, D. T.; Xu, J.; Cherry, J. H.; Urry, D. W.; Daniell, H. *Biotechnol. Lett.* **1995**, *17*, 745−750.
(17) Goeden-Wood, N. L.; Conticello, V. P.; Muller, S. J.; Keasling, J. D. *Biomacromolecules* **2002**, *3*, 874−879.
(18) Mandel-Gutfreund, Y.; Gregoret, L. M. *J. Mol. Biol.* **2002**, *323*, 453−461.
(19) Trudelle, Y. *Polymer* **1975**, *16*, 9−15.
(20) Brack, A.; Orgel, L. E. *Nature (London)* **1975**, *256*, 383−387.
(21) MacPhee, C. E.; Dobson, C. M. *J. Am. Chem. Soc.* **2000**, *122*, 12707−12713.
(22) Zhang, S.; Holmes, T.; Lockshin, C.; Rich, A. *PNAS* **1993**, *90*, 3334−3338.
(23) Klunk, W.; Jacob, R. F.; Mason, R. P. *Anal. Biochem.* **1999**, *266*, 66−76.
(24) Krimm, S.; Bandekar, J. In *Advances in Protein Chemistry*; Anfinsen, C. B., Edsall, J. T., Richards, F. M., Eds.; Harcourt Brace Jovanovich: New York, 1986; Vol. 38, pp 181−364.
(25) Greenfield, N. J. Personal communication.
(26) Greenfield, N.; Fasman, G. D. *Biochemistry* **1969**, *8*, 4108−4116.
(27) Zhang, S.; Lockshin, C.; Cook, R.; Rich, A. *Biopolymers* **1994**, *34*, 663−672.
(28) Zhang, S.; Rich, A. *PNAS* **1997**, *94*, 23−28.
(29) El-Agnaf, O. M. A.; Bodles, A. M.; Guthrie, D. J. S.; Harriott, P.; Irvine, G. B. *Eur. J. Biochem.* **1998**, *258*, 157−163.
(30) Lashuel, H. A.; LaBrenz, S. R.; Woo, L.; Serpell, L. C.; Kelly, J. W. *J. Am. Chem. Soc.* **2000**, *122*, 5262−5277.
(31) Choo, D. W.; Schneider, J. P.; Graciani, N. R.; Kelly, J. W. *Macromolecules* **1996**, *29*, 355−366.
(32) Chothia, C. *J. Mol. Biol.* **1973**, *75*, 295−302.
(33) Marqusee, S. B.; Baldwin, R. L. *PNAS* **1987**, *84*, 8898−8902.
(34) MacPhee, C. E.; Dobson, C. M. *J. Mol. Biol.* **2000**, *297*, 1203−1215.
(35) Khurana, R.; Uversky, V. N.; Nielsen, L.; Fink, A. L. *J. Biol. Chem.* **2001**, *276*, 22715−22721.
(36) Klunk, W.; Pettegrew, J. W.; Abraham, D. J. *J. Histochem. Cytochem.* **1989**, *37*, 1293−1297.
(37) Ashburn, T. T.; Han, H.; Mcguiness, B. F.; Lansbury, P. T. *Chem. Biol.* **1996**, *3*, 351−358.

(38) Demaimay, R.; Harper, J.; Gordon, H.; Weaver, D.; Chesebero, B.; Caughey, B. *J. Neuorchem.* **1998**, *71*, 2534−2541.
(39) Turnell, W. G.; Finch, J. T. *J. Mol. Biol.* **1992**, *227*, 1205−1223.
(40) Inouye, H.; Kirschner, D. A. *J. Struct. Biol.* **2000**, *130*, 123−129.
(41) Cooper, T. M.; Stone, M. O. *Langmuir* **1998**, *14*, 6662−6668.
(42) Vecchio, G.; Bossi, A.; Pasta, P.; Carrea, G. *Int. J. Peptide Protein Res.* **1996**, *48*, 113−117.
(43) Arrondo, J. L. R.; Muga, A.; Castersan, J.; Goni, F. M. *Prog. Biophys. Mol. Biol.* **1993**, *59*, 23−56.
(44) Nyrkova, I. A.; Semenov, A. N.; Aggeli, A.; Bell, M.; Boden, N.; McLeish, T. C. B. *Eur. Phys. J. B* **2000**, *17*, 499−513.
(45) Zurdo, J.; Guijarro, J. I.; Jimenez, J. L.; Saibil, H. R.; Dobson, C. M. *J. Mol. Biol.* **2001**, *311*, 325−340.
(46) Cardoso, I.; Goldsbury, C. S.; Muller, S. A.; Olivieri, V.; Wirtz, S.; Damas, A. M.; Aebi, U.; Saraiva, M. J. *J. Mol. Biol.* **2002**, *317*, 683−695.
(47) Aggeli, A.; Nyrkova, I.; Bell, M.; Harding, R.; Carrick, L.; McLeish, T. C. B.; Semenov, A. N.; Boden, N. *PNAS* **2001**, *98*, 11857−11862.
(48) Serpell, L. C. F. P.; Sunde, M. In *Methods in Enzymology: Amyloid, Prions, and other Protein AggregatesA*; Academic Press: San Diego, 1999; Vol. 309, pp 526−536.
(49) Chamberlain, A. K.; MacPhee, C. E.; Zurdo, J.; Morozova-Roche, L. A.; Hill, H. A. O.; Dobson, C. M.; Davis, J. J. *Biophys. J.* **2000**, *79*, 3282−3293.

MA025952Z